Accepted Manuscript

Synthesis and structure'activity'relationship of 3,4'Diaryl'1H'pyrrolo[2,3'b]pyridines as irreversible Inhibitors of mutant EGFR'L858R/T790M

Marcel Günther, Julian Laux, Stefan Laufer

PII: S0928-0987(18)30512-8
DOI: https://doi.org/10.1016/j.ejps.2018.11.021
Reference: PHASCI 4755

To appear in: *European Journal of Pharmaceutical Sciences*

Received date: 23 August 2018
Revised date: 26 October 2018
Accepted date: 19 November 2018

Please cite this article as: Marcel Günther, Julian Laux, Stefan Laufer , Synthesis and structure'activity'relationship of 3,4'Diaryl'1H'pyrrolo[2,3'b]pyridines as irreversible Inhibitors of mutant EGFR'L858R/T790M. Phasci (2018), https://doi.org/10.1016/j.ejps.2018.11.021

Synthesis and Structure-Activity-Relationship of 3,4-Diaryl-1*H*-pyrrolo[2,3-*b*]pyridines as irreversible Inhibitors of mutant EGFR-L858R/T790M

Marcel Günther[A], Julian Laux[A] and Stefan Laufer[A,B]

[A]*Eberhard-Karls University of Tübingen, Auf der Morgenstelle 8, 72076 Tübingen, Germany,* [B]*Corresponding author*

Abstract

The epidermal growth factor receptor (EGFR) is a well validated drug target for the treatment of non-small cell lung cancer. Here we present an optimization approach and preliminary structure-activity relationship for 1*H*-pyrrolo[2,3-*b*]pyridines as covalent irreversible mutant EGFR inhibitors. We synthesized a focused library to investigate the effect of different aromatic substituents in the 4-position of this scaffold, interacting with the gatekeeper. We determined the activity of the synthesized compounds mutant EGFR enzyme assays and determined the selectivity over the wild type.

Keywords: Medicinal chemistry, Synthesis, Anti-cancer, EGFR, Biological activity

1. Introduction

The development of epidermal growth factor receptor (EGFR) inhibitors for the treatment of non-small cell lung cancer (NSCLC) resulted in three generations of small molecular drugs in one decade (Figure 1).[1] EGFR represents a well-validated drug target for patients harboring so-called activating mutations.[2,3] These mutations lead to a highly increased level of EGF signaling independent from extracellular stimuli. This results in an aberrant equilibrium between pro-apoptotic and pro-survival signals in malignant cells. Because the survival of these abnormal cells is highly dependent on the EGFR signaling pathway, EGFR inhibition leads to a rapid inhibition of tumor cell growth *in vitro* and tumor shrinkage *in vivo*.[4-6] However, patients harboring wild type (wt) EGFR showed poor response rates under an anti

EGFR therapy. The most frequently observed activating mutation in NSCLC patients is the single amino acid exchange L858R, located on exon 21 that codes for the tyrosine kinase domain of EGFR.[2,7] First generation EGFR inhibitors like gefitinib (*N*-(3-chloro-4-fluorophenyl)-7-methoxy-6-(3-morpholinopropoxy)quinazolin-4-amine) are highly potent inhibitors of this particular kinase variant. However, during long-term treatment, most of the initially responding patients develop secondary resistances to first generation EGFR inhibitors. The secondary point mutation T790M is the leading cause for drug resistance in 60 % of NSCLC patients.[8,9] Second generation EGFR inhibitor afatinib ((S,E)-*N*-(4-((3-chloro-4-fluorophenyl)amino)-7-((tetrahydrofuran-3-yl)oxy)quinazolin-6-yl)-4-(dimethylamino)but-2-enamide) overcomes L858R/T790M resistance by a covalent irreversible interaction with the enzyme. Thus, this compound bears a reactive Michael acceptor group, an acrylamide, for the alkylation of a non-catalytic cysteine (Cys797).[10] Dose limiting toxicity compromised the clinical efficacy of afatinib. The potent inhibition of wt EGFR has been linked to the serious side effects of afatinib.[11,12] The recently FDA approved third generation EGFR inhibitor osimertinib (*N*-(2-((2-(dimethylamino)ethyl)(methyl)amino)-4-methoxy-5-((4-(1-methyl-1*H*-indol-3-yl)pyrimidin-2-yl)amino)phenyl)acrylamide) was designed to covalently inhibit L858R and L858R/T790M mutant EGFR, while sparing the wild type.[13] Osimertinib inhibits EGFR-L858R/T790M with subnanomolar IC_{50} values and the wt EGFR inhibition in the literature ranges from ~1 to 184 nM, depending on the assay format.[13-15] Even though dose limiting toxicity could be reduced for osimertinib when compared with afatinib, this third generation EGFR inhibitor still shows the typical wt associated EGFR inhibitor side effects in up to 30% of treated patients, namely skin rash, neutropenia, leukopenia and diarrhea.[16] The active metabolite AZ5104 (N-[2-[[2-(dimethylamino)ethyl]methylamino]-5-[[4-(1H-indol-3-yl)-2-pyrimidinyl]amino]-4-methoxyphenyl]-2-propenamide), which is the *N*-indole-demethylated derivative of osimertinib is less selective and displays a potent inhibitor of wt EGFR (15-fold more potent than osimertinib), which partially explains the adverse effects of osimertinib, observed in clinical trials. [17,18]

Here we present a rational design approach of novel covalent irreversible EGFR inhibitors towards improved activity and selectivity versus wild type, employing the 1*H*-pyrrolo[2,3-*b*]pyridine scaffold as a hinge binder. We previously described trisubstituted imidazoles bearing the 1*H*-pyrrolo[2,3-*b*]pyridine group to be a valuable scaffold to act as bidentate

hinge binders in EGFR (e.g. MJ-341 (N-(3-(4-(4-(4-fluorophenyl)-2-(3-hydroxypropyl)-1H-imidazol-5-yl)-1H-pyrrolo[2,3-b]pyridin-3-yl)phenyl)acrylamide), Figure 1).[19] We found the 3-position of the hinge binding heterocycle to be a suitable attachment point for a Michael acceptor linked via phenyl residues in order to covalently bind Cys797. MJ-277 (N-(3-(4-(4-(4-fluorophenyl)-2-(3-hydroxypropyl)-1H-imidazol-5-yl)-1H-pyrrolo[2,3-b]pyridin-3-yl)phenyl)acrylamide) served as a new hit compound for the development of EGFR inhibitors with decreased molecular weight when compared with the structure class of MJ-341 and promising biological activity. We could develop highly potent compounds with this chemotype for EGFR-L858R/T790M and for EGFR-L858R/T790M/C797S in the past.[19] However, we could not improve the selectivity over EGFR wild type. In the present work, we further synthesized a focused library of closely related compounds decorated with different substituents in the 4-position in order to improve the inhibitory activity and the selectivity over EGFR wild type. It has been recently shown that placing aromatic residues between the gatekeeper Met790 residue and Lys745 can be used to increase EGFR-L858R/T790M activity while maintaining selectivity versus wild type.[20] Docking predicted the 4-position of the 1*H*-pyrrolo[2,3-*B*]pyridine scaffold to be the most promising attachment point for substituents towards this direction (Figure 2). Covalent docking of 17 and 19 predicted a bidentate hinge-binding motif and orientation of the aromatic residues between Met790 and Lys745 but avoiding to fully occupy hydrophobic region I, which might be detrimental for selectivity. For 19, docking predicted an additional hydrogen bond between the protonated amine of Lys745 and the sulfonamide group (Figure 2B) that might be beneficial for inhibitory activity.

2. Materials and Methods

2.1 Compound synthesis and characterization

A detailed description of compound syntheses and characterization can be found in the supplementary information.

2.2 Biochemical characterization

Inhibition data (IC_{50}) against EGFR-wildtype, EGFR-L858R/T790M and EGFR-L858R/T790M/C797S as well as selectivity among targetable cysteine containing kinases (JAK3, MKK7, TEC, TXK, ITK, BTK wt, BMX, BLK, ERBB2 wt, EGFR wt, ERBB4) were conducted at Reaction Biology corp via commercial radiolabeled $^{33}P(ATP)$ kinase assays. IC_{50} values were measured in duplicates at 5 different concentration with 10-fold dilution steps starting from 5 µM. Staurosporine was tested as control compound in singlicate at 10 different concentrations with a 4-fold dilution starting at 20 µM. Inhibition of targetable cysteine containing kinases were performed at single concentrations (200 nM) in duplicates. A detailed description of the assay format is given in the literature[21,22].

3 Results and Discussion

3.1 Chemistry

For the synthesis of a focused library (scheme 1), we first converted commercially available 1*H*-pyrrolo[2,3-*B*]pyridine to the corresponding 7-*N*-oxide (**2**) using mCPBA (m-chloroperbenzoic acid).[23] Subsequent chlorination with methanesulfonyl chloride gave the 4-chloro derivative (**3**) in good yield. Next we iodinated the 3-position of the scaffold with I_2 under basic conditions. For the following Pd-catalyzed cross coupling reactions, we had to protect the nitrogen in 1-position of the 1*H*-pyrrolo[2,3-*B*]pyridine core. Thus, we introduced a SEM (trimethylsilylethoxymethyl) protective group by deprotonation with sodium hydride and nucleophilic substitution of SEM chloride. Initially this step yielded a regioisomeric mixture of the 1- and 7-SEM protected 1*H*-pyrrolo[2,3-*B*]pyridine **5**, which could be converted to the 1-regioisomere by stirring with a catalytic amount of SEM chloride at elevated temperature in acetonitrile. To install an aromatic linker, that should later bear the reactive Michael acceptor, we introduced the meta-nitrophenyl residue by means of Suzuki cross coupling reaction using 3-Nitrophenyl boronic acid in good yields. Next we either used Suzuki or Buchwald-Hartwig cross coupling reactions for carbon-carbon or carbon-nitrogen bond formations in the 4-position of the scaffold to yield intermediates **7a-i**. We converted the nitro group to the corresponding primary aromatic amine (**8a-i**) by heterogeneous catalysis using hydrogen and palladium on activated charcoal in excellent yields. Amide bond formation with acryloyl chloride under biphasic Schotten-Baumann conditions gave acrylamides **9a-i** in acceptable to excellent yields. SEM-deprotection was achieved using trifluoroacetic acid in

methylene chloride yielding compounds 10 – 15 and 22 - 24. For the synthesis of *N*-substituted indol-3-yl and pyrazol-3-yl derivatives (scheme 2), we first introduced the *N*-tosyl-protected heterocycles by Suzuki cross coupling reactions (**26a, b**). Selective deprotection with KOH in MeOH yielded the free NH heterocycles (**27a, b**), which could be substituted using sodium hydride and the corresponding alkyl halides or sulfonyl chlorides. Subsequent reduction of the nitro group followed by amide bond formation and SEM deprotection yielded final compounds 17 - 21. For the synthesis of 16, we introduced TIPS (triisopropylsilyl) protected indole by Suzuki cross coupling, followed by reduction of the nitro group, amide bond formation with acryloyl chloride and subsequent one step TIPS and SEM deprotection. Boronic acids or acid esters were synthesized by lithiation-borylation or Miyaura borylation approaches following literature procedures.[24]

3.2 Kinase Inhibition

We next determined the inhibitory activities of our synthesized compounds for the gefitinib resistant L858R/T790M EGFR mutant (Table 1) in an activity based ^{33}P(ATP) commercially available radiometric assay. [21,22] In this assay, the hit compound MJ-277 showed an IC_{50} value of 0.068 μM. To examine the potential of an interaction between R and the gatekeeper methionine of the EGFR L858R/T790M mutant, we synthesized compounds with varying substituents in this position. We have chosen more and less bulky aromatic residues as well as electron rich and poor analogues. Growing the size and spatial requirements from phenyl (10) to naphth-1-yl analogue 11 resulted in a significant drop of activity (1.27 μM) of over one order of magnitude. However, we could determine an IC_{50} value of 0.198 μM for the naphth-2-yl derivative 12, indicating that this substitution pattern is much better tolerated. These findings suggest that an annelated ring system might clash with the gatekeeper if the angle is too short, as it is for the naphth-1-yl derivative 11. And moreover, we could show with compound 12, that indeed these ring systems can be installed in the 1*H*-pyrrolo[2,3-*B*]pyridine 4-position in order to address the gatekeeper region. We next determined the influence of electron rich heterocycles (13 – 15) in this position. Compound 13 showed an IC_{50} value of 0.027 μM and a 3.6 fold increase of activity when compared with the phenyl analogue 10. We could even improve the activity with pyrazole bearing compounds 20 and 21 to IC_{50} values of 0.018 μM and 0.012 μM, respectively. The electron poor pyridine-4-yl derivative (22) showed a tremendous drop of

activity resulting in an IC_{50} value of 0.97 μM. Compared to the phenyl analogue (10) this represents an almost 10-fold decrease of activity, indicating the importance of electron density of these substituents. We could also improve the activity of 10 by installing the corresponding phenylamino residue (23), a more flexible substitution pattern, resulting in an IC_{50} value of 0.045 μM. However, we could not transfer this to the naphthyl-1-amine derivative (24) which showed a complete lack of inhibition. We next decorated the 1*H*-pyrrolo[2,3-*B*]pyridine scaffold with indol-3-yl substituents (17 – 19). The three *N*-substituted indole moieties improved the activity, in general. We determined an IC_{50} value of 0.060 μM for compound 16, bearing the unsubstituted indole as well as 0.014 μM and 0.042 μM for the *N*-isopropyl and *N*-methylsufonyl derivatives 18 and 19, respectively. The most potent compound (17) in this series showed an IC_{50} value very close to the resolution limit of the kinase assay of 0.001 μM. The kinase concentration (2 nM) used in the assays set a lower resolution limit of 1 nM to determine inhibitory activities quantitatively. With 17, we could achieve higher inhibitory activities than with our previously published highly optimized compound MJ-341, while reducing molecular weight.

3.3 Compound selectivity

To examine the compound's selectivity profile, we determined the inhibitory activities of selected compounds against EGFR wild type in an activity based $^{33}P(ATP)$ commercially available radiometric assay.[21,22] Table 2 shows the results of our tested compounds in an EGFR wt enzyme assay and the selectivity ratio for the double mutant EGFR-L858R/T790M over the wild type. Except compounds 11 and 16, most of our compound showed preference for the double mutant EGFR-L858R/T790M. For the most selective compound (12) we could determine a selectivity ratio of over 11. Nevertheless, this compound showed decreased inhibitory activity of 0.20 μM against EGFR-L858R/T790M. However, this assay setting was not suitable for the selectivity determination of the most potent compound 17 and osimertinib, because these compounds showed IC_{50} values below and close to the resolution limit of 0.001 μM. Interestingly 16 showed comparable IC_{50} values for the mutant and the wild type enzyme in the low nanomolar range. This indicates that this particular compound covalently binds to both tested proteins with some preference to the wild type. In order to obtain reliable IC_{50} values we modified the enzyme assays and tested compound 17 with an increased

concentration of ATP. At a 10 fold increased ATP concentration, compound 17 showed IC_{50} values of 0.002 μM and 0.012 μM against EGFR-L858R/T790M and EGFR-wt, respectively. We could determine a selectivity ratio of 6 with these modified assay conditions. To examine the influence of the covalent bond formation on the inhibitory activity, we tested selected compounds in a triple mutant EGFR-L858R/T790M/C797S enzyme assay. This enzyme lacks the non-catalytic cysteine 797 that is necessary for the covalent bond formation. We have recently shown, that this mutation can be overcome by the optimization of non-covalent reversible binding patterns of covalent irreversible EGFR inhibitors.[14,19,25] Because these compounds and osimertinib show only limited interactions with the ATP pocket besides the covalent bond formation, we expected a dramatic drop of activity when compared with the double mutant EGFR-L858R/T790M assay. As expected, all tested compounds showed a tremendous decrease of activity for the cysteine mutated protein. This indicates that our synthesized potent compounds covalently bind to the double mutant EGFR-L858R/T790M and that this interaction is the major contributor to the inhibitory activity. With an IC_{50} value of 1.3 μM, compound 17 showed low residual activity, due to reversible binding. However, 10 – 13 and 20 – 21 showed a drop of activity of up to over 500-fold. We also determined the selectivity of 13 and 17 in a panel of the ten kinases carrying a cysteine at the equivalent position. As depicted in Table 4, the most potent compound 17 showed over 70% inhibition for eight of these kinases. Compound 13 showed a more selective profile, inhibiting five other kinases. It is noteworthy that this compound shows selectivity within the ErbB kinase family, while 17 does inhibit these kinases.

4 Conclusion

In summary, we successfully developed EGFR-L858R/T790M inhibitors based on the 1*H*-pyrrolo[2,3-*B*]pyridine core as the hinge binding motif. We developed robust and modular synthetic routes to prepare 3,4-diaryl 1*H*-pyrrolo[2,3-*B*]pyridines. The most potent compound (17) showed an IC_{50} value of 0.001 μM in the gefitinib resistant EGFR-L858R/T790M enzyme assay and selectivity over the wild type. For the most selective compounds (12 and 13) we could determine over 10 fold selectivity for the mutant enzyme over the wild type, while 13 inhibits the EGFR-L858R/T790M in the low nanomolar range. In addition, we could show the influence of the covalent bond formation on the inhibitory activity by testing against the cysteine

MUTATED PROTEIN. WE HAVE SUCCESSFULLY SHOWN THE GREAT POTENTIAL OF THIS SCAFFOLD TOWARD EGFR INHIBITION. THIS NOVEL STRUCTURE CLASS COULD SERVE AS A NEW LEAD STRUCTURE FOR THE FURTHER DEVELOPMENT OF EITHER EGFR INHIBITORS OR POTENT INHIBITORS OF OTHER PROTEIN KINASE, CONTAINING TARGETABLE CYSTEINE RESIDUES AT AN EQUIVALENT POSITION.

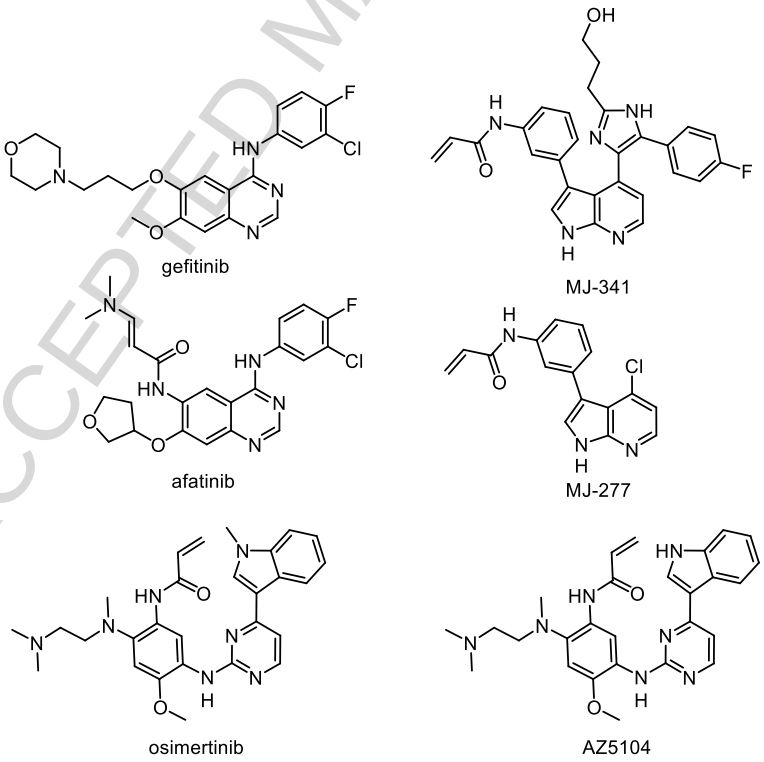

FIGURE 1: THREE GENERATIONS OF FDA APPROVED EGFR INHIBITORS (LEFT). HIT COMPOUNDS MJ-277 AND MJ-341 AND METABOLITE AZ5104 (RIGHT).

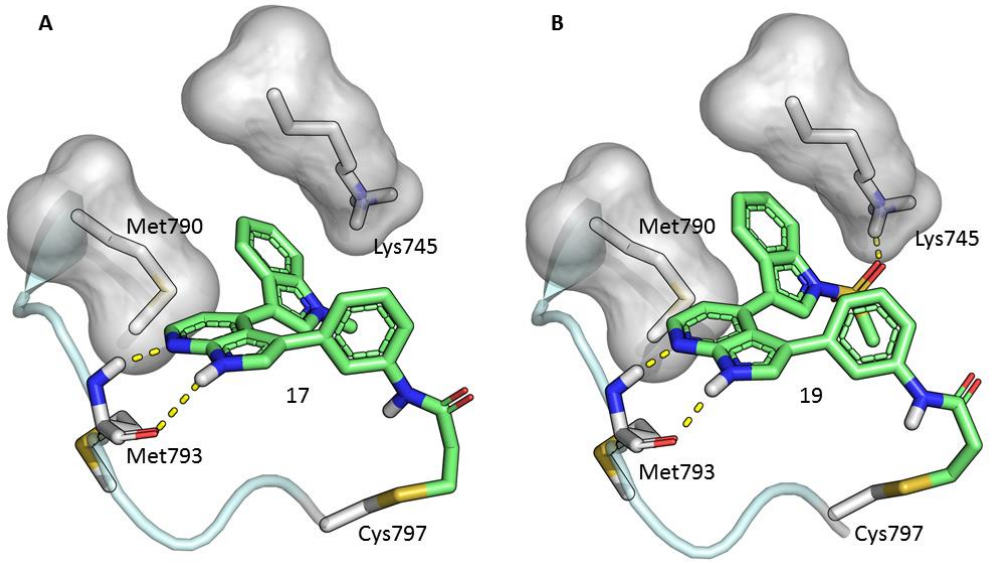

FIGURE 2: RATIONAL FOR THE SYNTHESIS OF A FOCUSED LIBRARY OF EGFR INHIBITORS. PREDICTED COVALENT BINDING MODES: A: DOCKING POSE OF 17 IN AN X-RAY STRUCTURE OF T790M MUTATED EGFR (PDB-CODE: 2JIU). B: DOCKING POSE OF 19 IN AN X-RAY STRUCTURE OF T790M MUTATED EGFR (PDB-CODE: 2JIU. PREDICTED HYDROGEN BONDS ARE DEPICTED AS DASHED YELLOW LINES.

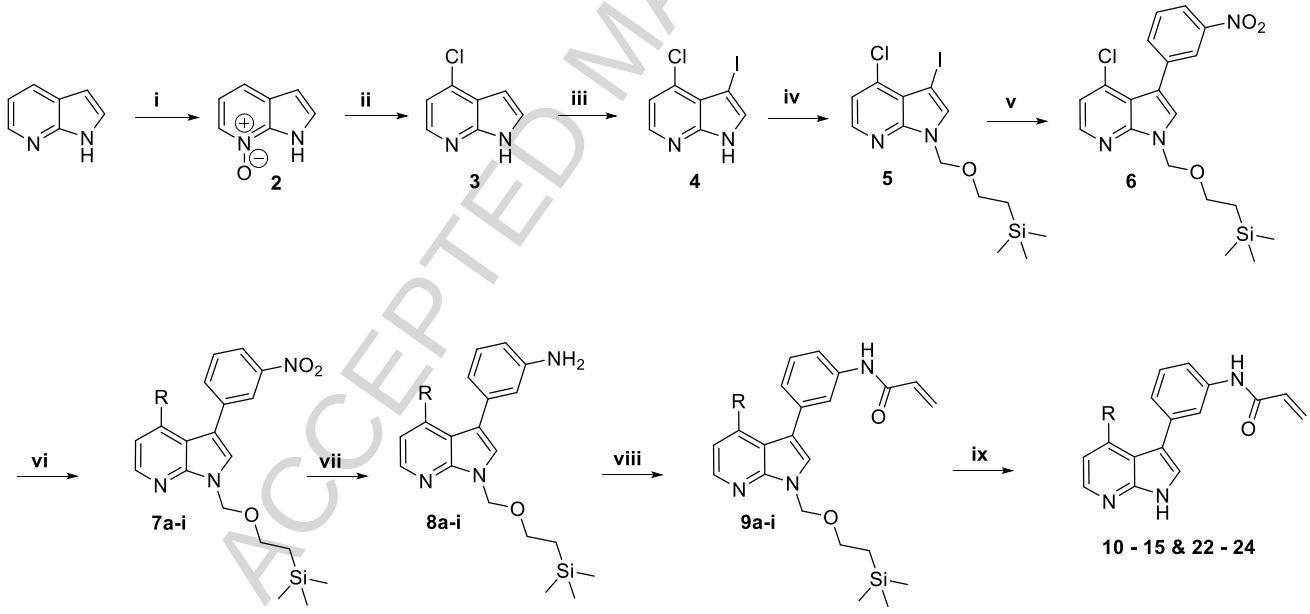

SCHEME 1: REAGENTS AND CONDITIONS: **I)**: M-CHLOROPERBENZOIC ACID, N-HEXANE, DIMETHOXYETHANE, RT, 3H, 62 %; **II)**: CH_3SO_2Cl, DMF, 75 °C, 8H, 62 %; **III)**: KOH (S), I_2, DMF, RT, 2H, 66 %; **IV)**: NAH, SEM-CL, TETRAHYDROFURAN, 50 °C, 2H, 88 %; **V)**: Na_2CO_3 (AQ), $Pd(PPh_3)_2Cl_2$, 3-NITROPHENYLBORONIC ACID, 1,4-DIOXANE, 40 °C, OVERNIGHT, 75-83 %; **VI)**: (H-I): Na_2CO_3 (AQ), SPHOS PD G_3, R-$B(OH)_2$, 1,4-DIOXANE, 50-87 % (A-G): K_2CO_3 (S), XPHOS PD G_4 ((2-DICYCLOHEXYLPHOSPHINO-2',4',6'-TRIISOPROPYL-1,1'-BIPHENYL)[2-(2'-METHYLAMINO-1,1'-

BIPHENYL)]-PALLADIUM(II) METHANESULFONATE) , R-NH_2, 1,4-DIOXANE, *T*-BUOH, 13-34 % (H,I); **VII)**: H_2, PD-C, ETOAC, RT, OVERNIGHT, 90-99 %; **VIII)**: $NaHCO_3$ (AQ), ACRYLOYL CHLORIDE, H_2O, TETRAHYDROFURAN, 0 °C, 30 MIN, 41-93 %; **IX)**: TRIFLUOROACETIC ACID, METHYLENE CHLORIDE, RT, OVERNIGHT, 43-83 %; A = PHENYL, B = NAPHTHALEN-1-YL, C = NAPHTHALEN-2-YL, D = FURAN-2-YL, E = THIOPHEN-3-YL, F = THIOPHEN-2-YL, G = PYRIDINE-4-YL, H = PHENYLAMINO, I = 1-NAPHTYLAMINO. SEM: TRIMETHYLSILYLETHOXYMETHYL.

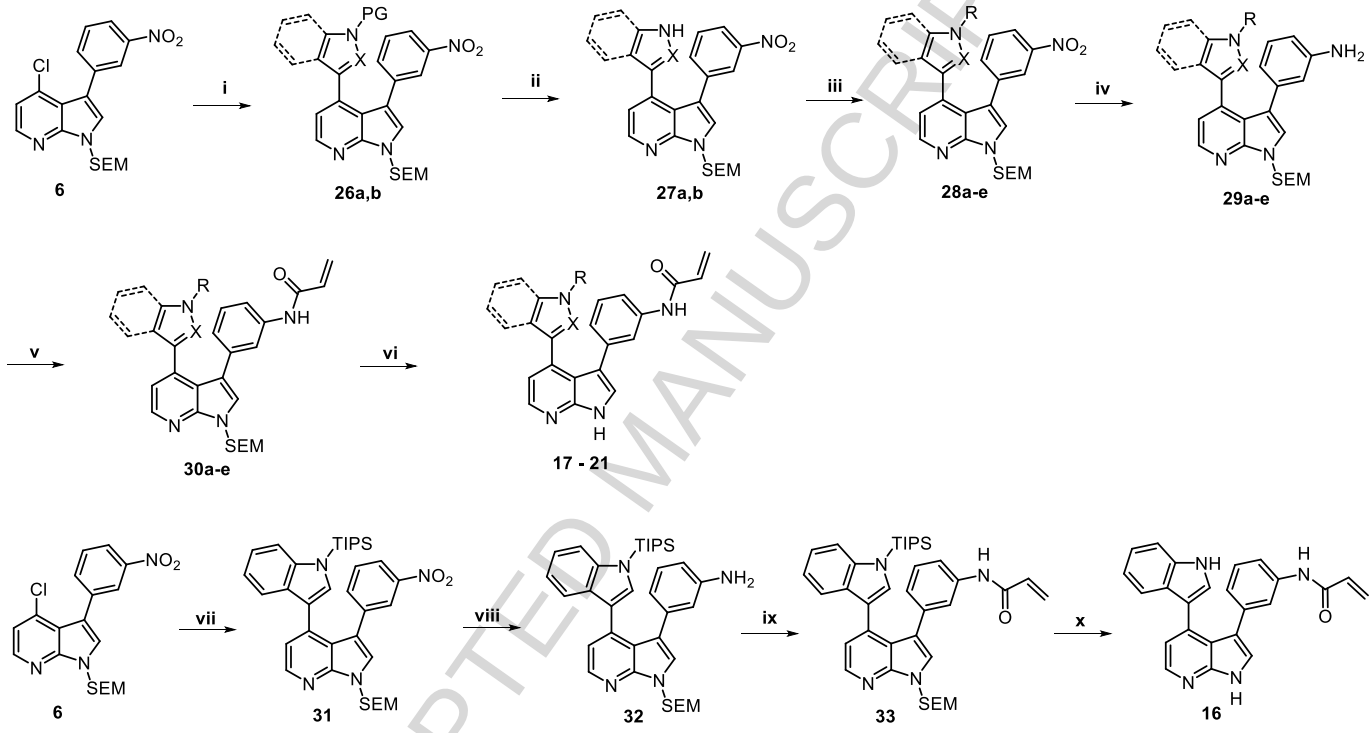

SCHEME 2: REAGENTS AND CONDITIONS: **I)** CORRESPONDING BORONIC ACID OR BORONIC ACID ESTER, SPHOS PD G_3 (2-DICYCLOHEXYLPHOSPHINO-2′,6′-DIMETHOXYBIPHENYL) [2-(2′-AMINO-1,1′-BIPHENYL)]PALLADIUM(II) METHANESULFONATE), Na_2CO_3, 1,4-DIOXANE /H_2O, 40°C, 6H, 68 – 74%; **II)** KOH, MEOH, RT, OVERNIGHT, 63 – 95%, **III)** NAH, R-X, TETRAHYDROFURAN, 0°C, 55 – 97 %, **IV)** H_2, PD/C, ETOAC, RT, OVERNIGHT, 85 – 99%, **V)** ACRYLOYL CHLORIDE, TETRAHYDROFURAN/H_2O, $NaHCO_3$, 0°C, 30 MIN, 54 – 92%, **VI)** TRIFLUOROACETIC ACID, METHYLENE CHLORIDE, $NaHCO_3$, 48 – 77%, **VII)** 3-(4,4,5,5-TETRAMETHYL-1,3,2-DIOXABOROLAN-2-YL)-1-(TRIISOPROPYLSILYL)-1*H*-INDOLE, SPHOS PD G_3, Na_2CO_3, 1,4-DIOXANE/H_2O, 30°C, OVERNIGHT, 50%, **VIII)** H_2, PD/C, ETOAC, RT, OVERNIGHT, 98%, **IX)** ACRYLOYL CHLORIDE, TETRAHYDROFURAN/H_2O, $NaHCO_3$, 0°C, 30 MIN, 90%, **X)** 1. TRIFLUOROACETIC ACID, METHYLENE CHLORIDE, 60°C OVERNIGHT, 49%. 26/27: A = INDOL-3-YL; PG = PHENYLSULFONYL, B = PYRAZOL-3-YL; PG

= TOSYL, 28/29/30: A = *N*-METHYLINDOL-3-YL, B = *N*-METHYLSULFONYLINDOL-3-YL, C = *N*-ISOPROPYLINDOL-3-YL, D = *N*-METHYLPYRAZOL-3-YL, E = *N*-METHYLSULFONYLPYRAZOL-3-YL

TABLE 1: IC_{50} VALUES IN AN EGFR-L858R/T790M KINASE ASSAY.

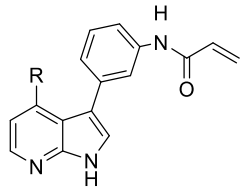

No.	R	IC50 EGFR-L858R/T790M [μM]	No.	R	IC50 EGFR-L858R/T790M [μM]
10		0.10	18	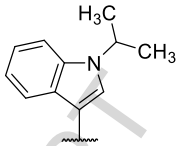	0.014
11	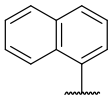	1.27	19	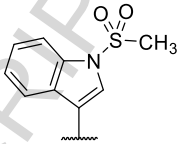	0.042
12	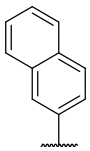	0.198	20	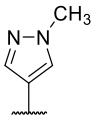	0.018
13		0.027	21	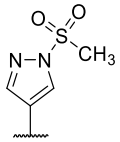	0.012
14		0.060	22	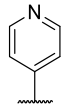	0.97
15		0.068	23	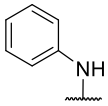	0.045
16	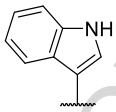	0.060	24	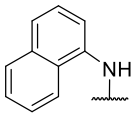	N.I.
17	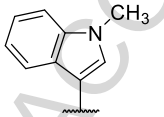	0.001	MJ-277	-	0.068
			MJ-341	-	0.002
			OSIMERTINIB	-	< 0.001*

* IC_{50} IS BELOW THE RESOLUTION LIMIT OF THE ASSAY (0.001 μM). N.I. NO INHIBITION AT THE HIGHEST COMPOUND CONCENTRATION OF 3 μM

TABLE 2: IC_{50} DETERMINATION AGAINST EGFR WILD TYPE AND SELECTIVITY RATIO

NO	IC_{50} EGFR WT [μM]	IC_{50} WT / IC_{50} LR/TM
10	0.425	4.3
11	0.242	0.2
12	2.26	11.4
13	0.291	10.8
14	0.571	9.5
15	0.725	10.7
16	0.004	0.1
17	0.003	3
MJ-277	0.525	7.7
MJ-341	< 0.001*	-
OSIMERTINIB	< 0.001*	-

* IC_{50} IS BELOW THE RESOLUTION LIMIT OF THE ASSAY (0.001 μM)

TABLE 3: IC_{50} DETERMINATION AGAINST EGFR-L858R/T790M/C797S

NO.	IC_{50} EGFR-L858R/T790M/C797S [μM]
10	N.I.
12	N.I.
13	N.I.
16	1.7
17	1.3
18	1.7
20	N.I.
21	N.I.

N.I. NO INHIBITION AT THE HIGHEST COMPOUND CONCENTRATION OF 3 AND 6 μM

TABLE 4: INHIBITION OF KINASES CARRYING A CYSTEINE AT AN EQUIVALENT POSITION

No.	17	13
KINASE	KINASE ACTIVITY [%]* @ 200 NM	
BLK	6	43
BMX/ETK	1	2
BTK	28	7
EGFR WILD-TYPE	4	69
ERBB2/HER2	14	85
ERBB4/HER4	0	66
ITK	14	42
JAK3	0	2
MKK7	67	73
TEC	44	23
TXK	1	0

*MEAN OF TWO EXPERIMENTS

GRAPHICAL ABSTRACT:

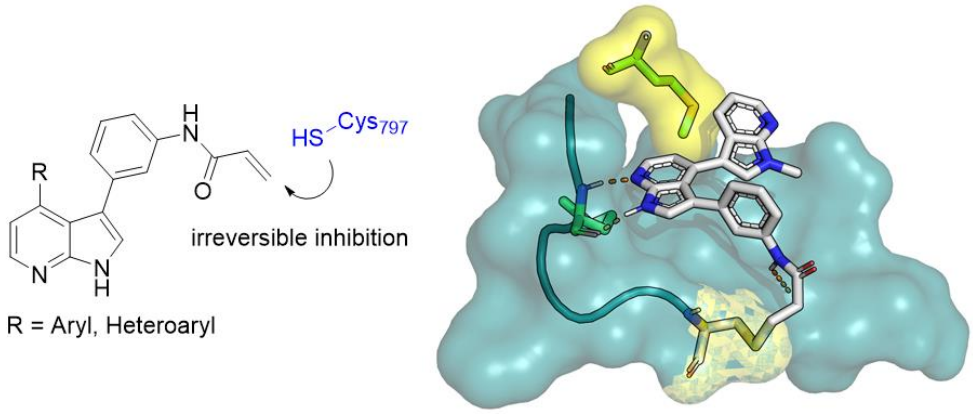

1. Russo, A., et al. A decade of EGFR inhibition in EGFR-mutated non small cell lung cancer (NSCLC): Old successes and future perspectives. *Oncotarget* **2015,** *6*, 26814-26825.

2. Lynch, T. J., et al. Activating mutations in the epidermal growth factor receptor underlying responsiveness of non-small-cell lung cancer to gefitinib. *N Engl J Med* **2004,** *350*, 2129-2139.

3. Gazdar, A. F. Activating and resistance mutations of EGFR in non-small-cell lung cancer: role in clinical response to EGFR tyrosine kinase inhibitors. *Oncogene* **2009,** *28 Suppl 1*, S24-31.

4. Pao, W., et al. EGF receptor gene mutations are common in lung cancers from "never smokers" and are associated with sensitivity of tumors to gefitinib and erlotinib. *Proc Natl Acad Sci U S A* **2004,** *101*, 13306-13311.

5. Takeda, M., et al. Survival outcome assessed according to tumor response and shrinkage pattern in patients with EGFR mutation-positive non-small-cell lung cancer treated with gefitinib or erlotinib. *J Thorac Oncol* **2014,** *9*, 200-204.

6. Juchum, M., et al. Fighting cancer drug resistance: Opportunities and challenges for mutation-specific EGFR inhibitors. *Drug Resist Updat* **2015,** *20*, 12-28.

7. Kawahara, A., et al. Molecular diagnosis of activating EGFR mutations in non-small cell lung cancer using mutation-specific antibodies for immunohistochemical analysis. *Clin Cancer Res* **2010,** *16*, 3163-3170.

8. Pao, W., et al. Acquired resistance of lung adenocarcinomas to gefitinib or erlotinib is associated with a second mutation in the EGFR kinase domain. *PLoS Med* **2005,** *2*, e73.

9. Yu, H. A., et al. Analysis of tumor specimens at the time of acquired resistance to EGFR-TKI therapy in 155 patients with EGFR-mutant lung cancers. *Clin Cancer Res* **2013,** *19*, 2240-2247.

10. Kwak, E. L., et al. Irreversible inhibitors of the EGF receptor may circumvent acquired resistance to gefitinib. *Proc Natl Acad Sci U S A* **2005,** *102*, 7665-7670.

11. Katakami, N., et al. LUX-Lung 4: a phase II trial of afatinib in patients with advanced non-small-cell lung cancer who progressed during prior treatment with erlotinib, gefitinib, or both. *J Clin Oncol* **2013,** *31*, 3335-3341.

12. Miller, V. A., et al. Afatinib versus placebo for patients with advanced, metastatic non-small-cell lung cancer after failure of erlotinib, gefitinib, or both, and one or two lines of chemotherapy (LUX-Lung 1): a phase 2b/3 randomised trial. *Lancet Oncol* **2012,** *13*, 528-538.

13. Cross, D. A., et al. AZD9291, an irreversible EGFR TKI, overcomes T790M-mediated resistance to EGFR inhibitors in lung cancer. *Cancer Discov* **2014,** *4*, 1046-1061.

14. Gunther, M., et al. Trisubstituted Pyridinylimidazoles as Potent Inhibitors of the Clinically Resistant L858R/T790M/C797S EGFR Mutant: Targeting of Both Hydrophobic Regions and the Phosphate Binding Site. *J Med Chem* **2017,** *60*, 5613-5637.

15. Finlay, M. R., et al. Discovery of a potent and selective EGFR inhibitor (AZD9291) of both sensitizing and T790M resistance mutations that spares the wild type form of the receptor. *J Med Chem* **2014,** *57*, 8249-8267.

16. Lamb, Y. N.; Scott, L. J. Osimertinib: A Review in T790M-Positive Advanced Non-Small Cell Lung Cancer. *Target Oncol* **2017,** *12*, 555-562.

17. Gao, X., et al. The safety and efficacy of osimertinib for the treatment of EGFR T790M mutation positive non-small-cell lung cancer. *Expert Rev Anticancer Ther* **2016,** *16*, 383-390.

18. Chu, C. Y., et al. Osimertinib: A Novel Dermatologic Adverse Event Profile in Patients with Lung Cancer. *Oncologist* **2018,** *23*, 891-899.

19. Juchum, M., et al. Trisubstituted Imidazoles with a Rigidized Hinge Binding Motif Act As Single Digit nM Inhibitors of Clinically Relevant EGFR L858R/T790M and L858R/T790M/C797S Mutants: An Example of Target Hopping. *J Med Chem* **2017,** *60*, 4636-4656.

20. Tomassi, S., et al. Indazole-Based Covalent Inhibitors To Target Drug-Resistant Epidermal Growth Factor Receptor. *J Med Chem* **2017,** *60*, 2361-2372.

21. Duong-Ly, K. C.; Peterson, J. R. A high-throughput radiometric kinase assay. *Methods Mol. Biol.* **2016,** *1360*, 87-95.

22. Anastassiadis, T., et al. Comprehensive assay of kinase catalytic activity reveals features of kinase inhibitor selectivity. *Nat Biotechnol* **2011,** *29*, 1039-1045.

23. Gehringer, M., et al. Solution-phase parallel synthesis of ruxolitinib-derived Janus kinase inhibitors via copper-catalyzed azide-alkyne cycloaddition. *ACS Comb Sci* **2015,** *17*, 5-10.

24. Chao, W. R., et al. Computer-aided rational drug design: a novel agent (SR13668) designed to mimic the unique anticancer mechanisms of dietary indole-3-carbinol to block Akt signaling. *J Med Chem* **2007,** *50,* 3412-3415.

25. Gunther, M., et al. Lung Cancer: EGFR Inhibitors with Low Nanomolar Activity against a Therapy-Resistant L858R/T790M/C797S Mutant. *Angew Chem Int Ed Engl* **2016,** *55,* 10890-10894.